Structure Changes in Hemoglobin upon Deletion of C-Terminal Residues, Monitored by Resonance Raman Spectroscopy†

Daojing Wang and Thomas G. Spiro*

Department of Chemistry, Princeton University, Princeton, New Jersey 08544

Received February 5, 1998; Revised Manuscript Received April 13, 1998

ABSTRACT: Loss of C-terminal residues in hemoglobin raises oxygen affinity and reduces both cooperativity and the Bohr effect. These functional changes are expected from the loss of C-terminal salt bridges, which are seen crystallographically to stabilize the T quaternary structure. Ultraviolet resonance Raman (UVRR) difference spectroscopy confirms that the strength of the T state contacts is diminished when the C-terminal and also the penultimate residues are removed chemically. Deoxy minus CO difference signals arising from the Trpβ37−Aspα94 and Tyrα42−Aspβ99 H bonds at the $\alpha_1\beta_2$ subunit interface are diminished, and at pH 9, the difference spectra reveal a shift to the R quaternary structure. These effects are small for desHisβ146 Hb and large for desArgα141 Hb, consistent with the order of functional changes. In addition, the H bond between the A and E helices is strengthened by removal of Argα141 and is further strengthened when the effector molecule IHP (inositol hexaphosphate) is added to deoxy-desArgα141 Hb or when its pH is lowered to 5.8. This effect is attributed to the loss of the C-terminal anchor of the α chain H helix, which supports the F and A helices. The β chain is not as sensitive because it has extra F−H interhelix H bonds. Removal of both Hisβ146 and Tyrβ145 produce UVRR changes which are intermediate between desHisβ146 and desArgα141 Hb, although the functional consequences are greater than for desArgα141 Hb. Removal of Tyrα140 as well as Argα141 abolishes cooperative binding as well as the Bohr effect, and the UVRR difference signals are also lost, suggesting that quaternary constraints are removed in both the T and the R states. When the ∼220 cm^{-1} iron−histidine stretching vibration of the deoxy-proteins is examined, using Raman excitation in resonance with the heme Soret band, the frequency is observed to diminish toward that of deoxyHb A (215 cm^{-1}) as the pH is lowered and IHP is added and to increase toward a completely relaxed value (223 cm^{-1}) as the pH is raised to 9. The relaxation is in the same order as the functional perturbations: desHisβ146 < desArgα141 < desHisβ146−Tyrβ145 < desArgα141−Tyrα140. However, even desArgα141−Tyrα140 Hb shows significant reduction in the Fe−His frequency as IHP is added at low pH. The Fe−His frequency is sensitive to both tertiary and quaternary structure changes and is a global indicator of forces at the heme. The order of affinity changes can be understood on the basis of the number of stabilizing H bonds between the F and H helices. Titration curves of the Fe−His frequency against pH are not sigmoidal, consistent with a multiplicity of contributions to the Bohr effect.

As part of a program to probe structure and dynamics in hemoglobin (Hb)[1] with vibrational spectroscopy (*1*−*5*), we report new results on human Hb which has been altered chemically by removal of the C-terminal residues Argα141 and Tyrα140 from the α chains and Hisβ146 and Tyrβ145 from the β chains. Perutz long ago pointed out the importance of the C-termini to the quaternary structure of Hb and investigated the functional consequences of their removal (*6*). The C-termini are located at either edge of the critical $\alpha_1\beta_2$ interface, where most of the quaternary rearrangement occurs between the T and R states (Figures 1 and 2). They form salt bridge and H-bond contacts across this interface in the T state, which are broken in the R state (*7*−*10*). Removal of these residues increases the oxygen affinity of Hb, and reduces the binding cooperativity (Table 1) (*11*−*25*). However, the deoxy forms still crystallize in the lattice of unmodified deoxy Hb (except when both Argα141 and Hisβ146, or both Argα141 and Tyrα140 are removed) (*19*), supporting the idea that the loss of the salt bridges destabilizes the T state, relative to the R state, without significantly altering the T and R structures themselves. Nevertheless, the forces favoring one or the other of these structures are expected to be altered, and these forces can be probed by vibrational spectroscopy.

Resonance Raman spectroscopy has been useful in this application because of the selective enhancement of chromophore vibrations provided by resonance of the laser

† This work was supported by NIH Grant GM25158 from the National Institute of General Medical Sciences.

* To whom correspondence should be addressed.

[1] Abbreviations: Hb, hemoglobin; HbA, adult human hemoglobin A; desArgα141 Hb, HbA with the last residue (Argα141) of α chains deleted; desArgα141-Tyrα140 Hb, HbA with the last two residues (Argα141 and Tyrα140) of α chains deleted; desHisβ146 Hb, HbA with the last residue (Hisβ146) of β chains deleted; desHisβ146-Tyrβ145 Hb, HbA with the last two residues (Hisβ146 and Tyrβ145) of β chains deleted; $\alpha_1\beta_2$, the interface between α_1 and β_2 subunits; $\alpha_2\beta_1$, the interface between α_2 and β_1 subunits; UVRR, ultraviolet resonance Raman; Vis-RR, visible resonance Raman; IHP, inositol hexaphosphate; ESMS, electrospray mass spectroscopy.

S0006-2960(98)00295-5 CCC: $15.00
Published on Web 06/26/1998

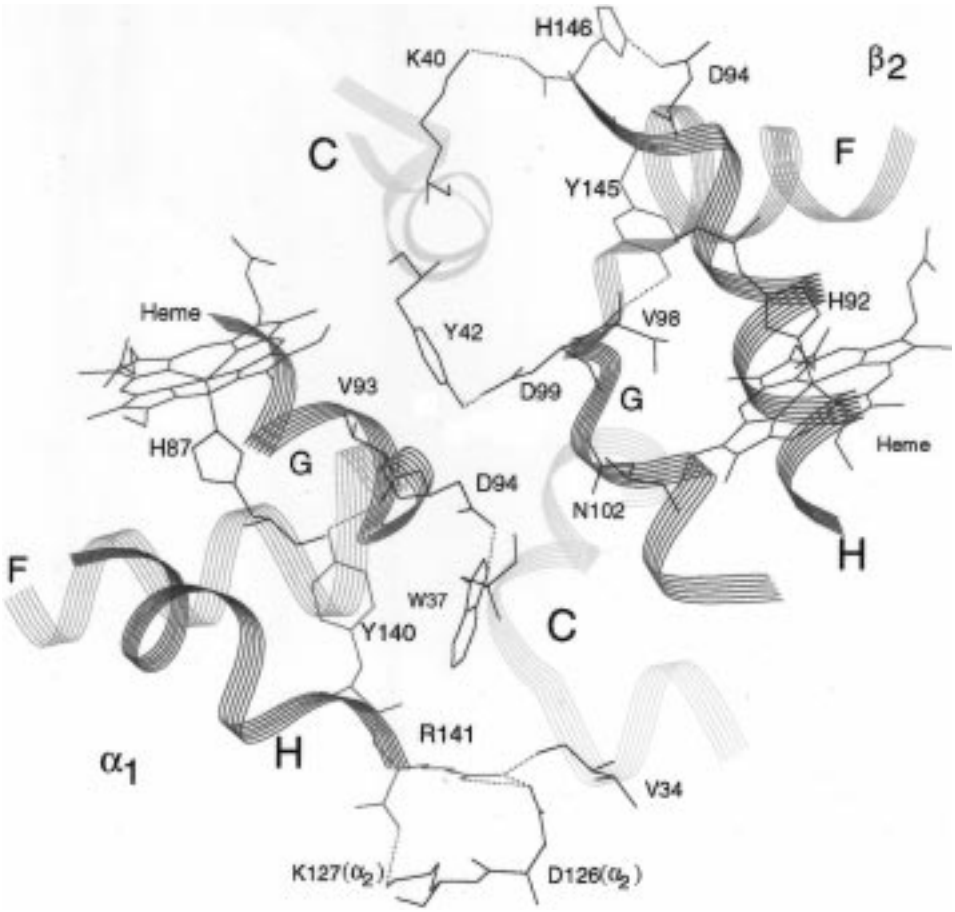

FIGURE 1: Ribbon diagram showing T-state contacts at the $\alpha_1\beta_2$ interface, the adjacent helices, and the heme groups. The C-terminal residues which are removed chemically are shown in red: Hisβ146 H bonds to Aspβ94 and forms a salt-bridge with Lysα40, while Tyrβ145 H bonds to Valβ98; Argα141 H bonds to Valβ34 and forms salt-bridges with Aspα126 and Lysα127 of the α_2 chain, while Tyrα140 H bonds to Valα93 [coordinates from PDB file 2HHB (*10*)].

Table 1: Functional Properties of Modified Hbs

	oxygen affinity $(Po_2)_{1/2}$ (mm Hg)	cooperativity (Hill coefficient) (n)	Bohr effect (H^+/per heme)	Initial CO binding rate constant ($M^{-1}\ s^{-1} \times 10^{-5}$)
HbA	9.2, pH 7.0 (*11*)	3.1, pH 7.0 (*12*)	0.48, pH 7.4 (*13*)	1.67, pH 7.0 $T = 20$ °C (*14*)
desHisβ146	2.5, pH 7.0 (*11*)	2.6, pH 7.0 (*12*)	0.23, pH 7.0 (*11*)	8.0, pH 7.0 $T = 20$ °C (*15*)
desArgα141	1.35, pH 6.8 (*16*)	2.0, pH 7.0 (*12*)	0.26, pH 7.4 (*13*)	12.2, pH 7.0 $T = 20$ °C (*14*)
desHisβ146−Tyrβ145	0.44, pH 7.4 (*17*)	1.2, pH 7.4 (*17*)	$^1/_3$ of normal magnitude, pH 7.4 (*18*)	40.0, pH 7.0 $T = 20$ °C (*18*)
desArgα141−Tyrα140	0.34, pH 7.3 (*13*)	1.0, all pHs (*12*)	no Bohr effect (*12, 19*) 0.07, pH 7.2 (*13*)	NA[a]
α chains	0.46, pH 7.0 (*20*)	1 (*21*)	0 (*21*)	45.8, pH 7.0 $T = 20$ °C (*20*)
β chains	0.40, pH 7.0 (*20*)	1 (*21*)	0 (*21*)	45.5, pH 7.0 $T = 20$ °C (*20*)
$\alpha\beta$ dimers	same as isolated α and β chains, pH 7.4 (*22*)	1 (*22*)	<0.1, around pH 7 (*23*)	NA[a]

[a] NA: not available.

excitation with electronic transitions of the molecule under study. In the case of Hb, excitation in the visible region of the spectrum enhances vibrations of the heme group and its ligands (*26*−*28*), while excitation in the ultraviolet region enhances vibrations of the aromatic side chains of the protein (*29*, *30*). The aromatic signals have been assigned for Hb, and markers of tertiary and quaternary interactions have been identified (*1*−*3*, *5*). These markers help us to characterize the changes induced by the C-terminal deletions. In addition, we can correlate these changes with the strength of the bond from the proximal histidine residue to the Fe atom, which is the single bond between the protein and the heme group. Its strength can be monitored via the frequency of the Fe−His stretching vibration, which is a prominent feature of the deoxy-heme RR spectrum obtained with visible excitation (*26*).

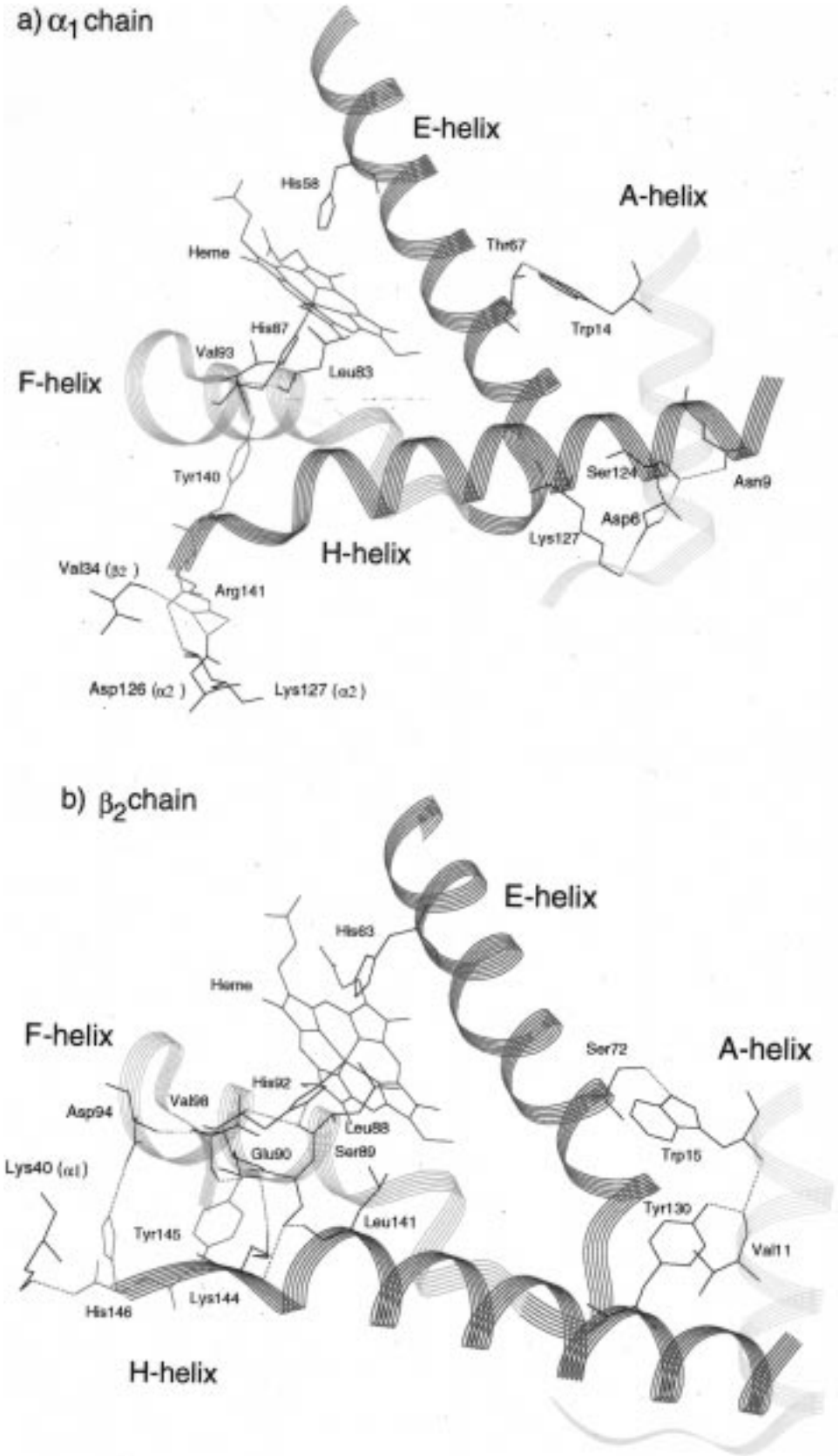

FIGURE 2: Ribbon diagram of the deoxy α and β chains, showing the heme held between the E and F helices, as well as the A−E, A−H, and F−H interhelix H bonds, and the C-terminal anchor. (a) α chain. (b) β chain [coordinates from PDB file 2HHB (*10*)].

MATERIALS AND METHODS

Hemoglobin Constructs. Adult human hemoglobin A (HbA) was prepared and purified from fresh blood following standard procedures (*31*). The red blood cells were exposed to CO, separated by centrifugation in NaCl solution (9 g/L), and subsequently disrupted by dilution in deionzied-distilled water. Membrane fragments were centrifuged out, and the

HbCO supernatant was stripped of organic phosphates and other ions by passing through ion retardation resin AG11A8 (Bio-Rad) and a mixed bed deionizing column with AG501-X8(D) (Bio-Rad). The protein was stored frozen at 77 K as the CO derivative in pH 8.5 Tris buffer containing 0.5 mM EDTA. To eliminate traces of Met Hb, the stock solution was saturated with CO and treated with a small amount of sodium hydrosulfite, which was immediately removed by gel filtration on a G-25 column. Alternatively, a CM-52 ion-exchange column was used to remove the Met form. Solutions of 0.25 mM deoxyHb (1 mM in heme) at different pH values were generated by irradiating the deoxygenated HbCO solution with visible light at 4 °C and blowing pure nitrogen over it. HbCO solutions were prepared by exposing the deoxyHb solution to 1 atm CO to ensure the same concentration as the deoxy Hb solution. Polyacrylamide gel electrophoresis (*32*) and absorption spectra (*31*) were used to test the purity.

DesArgα141 Hb and desHisβ146−Tyrβ145 Hb were prepared by digestion of HbCO with carboxypeptidase B and carboxypeptidase A, respectively (*33*). DesArgα141−Tyrα140 Hb was made by recombination of normal β chains with desArgα141−Tyrα140 α chains. DesHisβ146 Hb was prepared by recombination of α chain with desHisβ146 β chain. DesArgα141 α chain was separated from desArgα141 Hb, then desArgα141−Tyrα140 α chain was prepared by digestion of desArgα141 α chain with carboxypeptidase A (*33*). The desHisβ146 β chain was prepared by digestion of β chain with carboxypeptidase B. The amount of carboxypeptidase B was 5-fold higher than that in ref *33*, and the yield of the product was increased to 70%. The modified Hbs were further purified by gel filtration on a Sephadex G-25 (fine) column and chromatography on a CM-52 ion-exchange column. The linear gradient of the eluent was modified to improve efficiency in the purification of the products; a pH 6.3 linear salt gradient (500 mL of 0.01 M sodium phosphate to 750 mL of 0.1 M sodium phosphate) was used for desArgα141 Hb, while a pH 5.5 linear salt gradient (750 mL 0.01 M sodium phosphate to 500 mL of 0.01 M sodium phosphate + 0.5 M NaCl) was used for desHisβ146−Tyrβ145 Hb. DesHisβ146 Hb and desArgα141−Tyrα140 Hb were purified as described in the literature (*33*).

α and β chains of normal and modified Hbs were separated following the procedure of Bucci et al. (*34*−*35*) as modified by Yip et al. (*36*). The tetramers were reassembled following the method of Ikeda-Saito et al. (*37*).

Purity and homogeneity of the products were monitored by electrospray mass spectrometry (ESMS) and 7.5% polyacrylamide gel electrophoresis under nondenaturing conditions.

UV Resonance Raman Spectroscopy. UVRR spectra were obtained with the spectrometer described previously, with minor changes (*1*, *5*). Laser excitation at 229 nm was provided by a frequency doubled Innova 300 argon ion laser (Coherent). The laser power at the sample was about 0.35 mW. The scattered light was collected with an *f*/1 paraboloid mirror in backscattering geometry and focused with an *f*-matching lens into a 1.26 m single spectrometer (SPEX 1269) with an intensified diode array detector. Proteins were 1 mM in heme. Different pHs were attained by using 50 mM Bis-Tris (pH 5.8, pH 6.5), 50 mM sodium phosphate (pH 7.4), and 50 mM Tris (pH 9.0) buffers. All buffer solutions contained 0.5 mM EDTA. In experiments performed with IHP (inositol hexaphosphate), a 10-fold molar excess with respect to Hb tetramer was added. The IHP solutions were adjusted to pH 7.0 with pure H_3PO_4. Sample volumes of 0.5 mL (containing 0.2 M $NaClO_4$ as a frequency and intensity standard) were contained in a 5 mm quartz EPR tube, which was spun around a stationary helical wire (*1*). A nitrogen atmosphere was maintained over the samples by flowing N_2 into the sample tube through a thin stainless steel tube. The cooled N_2 gas kept the sample temperature between 10 and 15 °C. Spectral acquisitions were carried out in 30 min increments. Difference spectra were generated by using the perchlorate band at 934 cm^{-1} as the internal intensity standard.

Table 2: Electrospray Mass Spectrometry (ESMS) Masses (daltons) of Modified Hbs

	α chain	β chain
HbA	15 125.6	15 865.6
calcd	15 126	15 867
desArgα141	14 970.3	15 867.3
calcd	14 970	15 867
desArgα141−Tyrα140	14 806.3	15 865.1
calcd	14 807	15 867
desHisβ146	15 127.5	15 730.0
calcd	15 126	15 730
desHisβ146−Tyrβ145	15 126.4	15 564.8
calcd	15 126	15 567

Visible Resonance Raman Spectroscopy. A continuous wave Liconix helium−cadmium (He−Cd) laser was used to provide 441.6 nm excitation. The laser power at the sample was about 10 mW. Samples were contained in a 5 mm glass NMR tube, which was positioned in a backscattering geometry and kept spinning during laser illumination. The scattered light was detected with a SPEX 1877 triplemate spectrograph equipped with a 2400 groove/mm grating and an intensified diode array detector (Princeton Instruments). The spectra were obtained in 20 min acquisitions.

RESULTS

Authentication of the Modified Hbs. Electrospray mass spectra (ESMS) gave the expected masses of intact and modified Hb chains, within experimental error (Table 2). Under the high-voltage electric field of ESMS, the Hb tetramer dissociates into α and β chains, and the heme groups are expelled. Thus, the calculated masses for α and β chains in normal Hb are 15 126 and 15 867, respectively. The 7.5% polyacrylamide gel electrophoresis pattern (not shown) under nondenaturing conditions was the same for CO forms of HbA, desHisβ146, and desHisβ146−Tyrβ145, but different from desArgα141 HbCO and desArgα141−Tyrα140 HbCO. The approximately 10% greater mobility for these two modified Hbs is due to their extra negative charge at pH 8.8. Deletion of Hisβ146 and Tyrβ145 does not affect mobility under the gel electrophoresis conditions used. Thus, the purity and homogeneity of the modified Hbs were verified.

UVRR Spectra and Difference Spectra. The modified hemoglobins gave high quality UVRR spectra (Figure 3), comparable to that obtained for native Hb A. With 229 nm excitation, the enhanced Raman bands arise from tyrosine

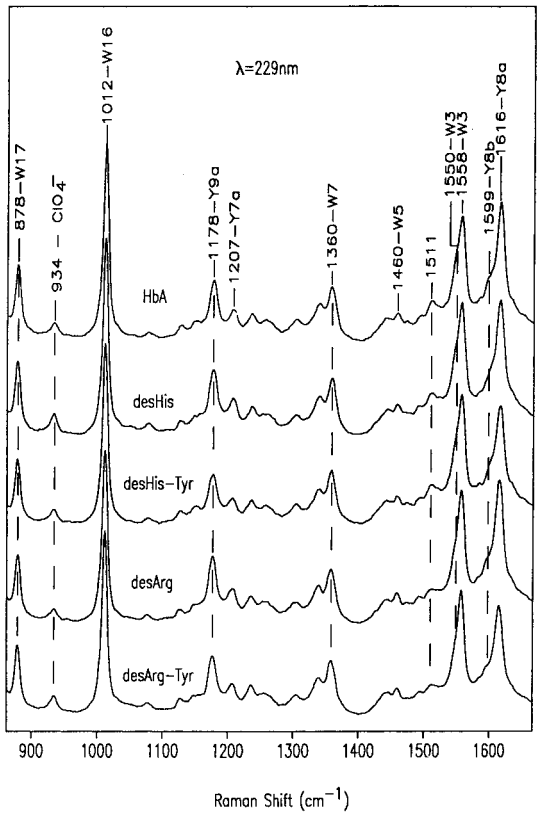

FIGURE 3: UVRR spectra excited at 229 nm of native and modified Hbs (deoxy forms, 1 mM in heme, pH 6.5). The top spectrum is labeled with Raman shifts and mode assignments (W = Trp modes, Y = Tyr modes). Separate positions are indicated for W3 from Trpβ37 (1548 cm^{-1}) and Trpα14/β15 (1558 cm^{-1}) (*1*, *5*).

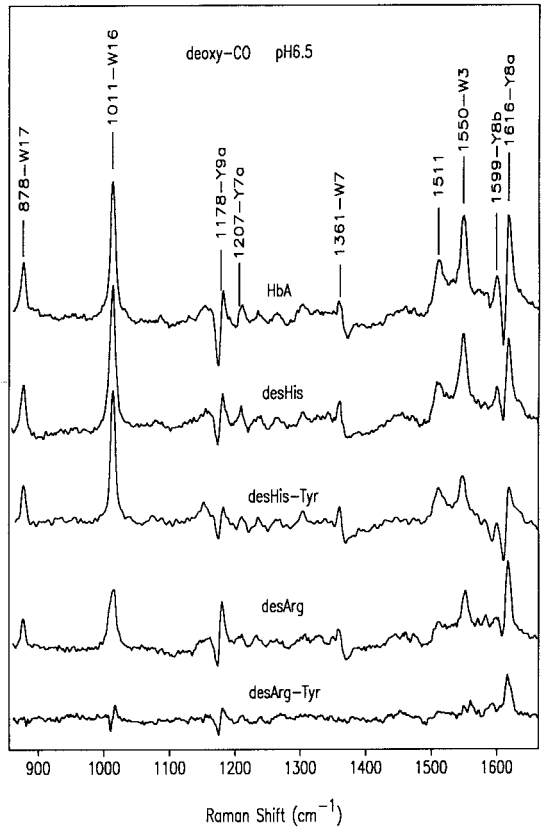

FIGURE 4: Deoxy minus CO difference UVRR spectra for native and modified Hbs at pH 6.5.

and tryptophan residues (*1*); the mode labels (Y for Tyr, W for Trp) (*29*) are indicated in the figure. The spectra are all very similar, and the obvious differences are limited to the intensities of the Tyr bands, which are lower for the constructs in which the penultimate Tyr residues have been removed, desHisβ146−Tyrβ145 and desArgα141−Tyrα140. There are six tyrosine residues per $\alpha\beta$ dimer, and deletion of one of them should lower the Tyr intensities by about 15%, consistent with the observed spectra.

More subtle variations are seen in the deoxy minus CO difference spectra, which are compared at pH 6.5 in Figure 4. The sources of the difference signals have been analyzed for Hb A, using isotopic substitution (*5*). The Trp difference bands arise almost entirely from Trpβ37, which donates a H bond to the carboxylate side chain of Aspα94, across the $\alpha_1\beta_2$ interface, in the T state (Figure 1). This H bond is broken in the R state and is replaced by a weaker intrachain H bond to the backbone carbonyl of Asn β102 (*7*−*10*). The two other Trp residues, α14 and β15, do not alter their H-bond partner (Figure 2), and contribute very little to the T − R difference spectra (*1*, *5*). Consequently, the W3 difference band is at 1550 cm^{-1}, the frequency assigned to Trp β37, and there is no difference intensity at 1558 cm^{-1}, the W3 frequency of Trpα14 and β15, which dominate the W3 band envelope in the parent spectra (Figure 3). The frequency is lowered specifically for Trpβ37 because of a large dihedral angle about the bond connecting the indole ring to the backbone (*1*, *38*).

When the C-terminal residues are deleted, the Trp difference bands are unaltered in frequency but diminish in intensity in the order desHisβ146 > desHisβ146−Tyrβ145 > desArgα141 > desArgα141−Tyrα140. To obtain a more quantitative indication of this trend, we deconvoluted the parent spectra and determined the band areas for the three strong Trp bands, W3, W16 and W17 (Table 3). The T vs R intensity increase in Hb A is about 20% for W16 and W17 and about 40% for W3. These differences are essentially unaltered for desHisβ146, but diminish progressively for desHisβ146−Tyrβ145 and desArgα141, and essentially disappear for desArgα141−Tyrα140.

Table 3: Curvefitting of Trp W17, W16, and W3 Bands in the 229-nm-Excited UVRR Spectra at pH 6.5[a]

	W17 (879 cm^{-1}) $\Delta I/I_{CO}$ (%)	W16 (1012 cm^{-1}) $\Delta I/I_{CO}$ (%)	W3 (Trpβ37, 1549 cm^{-1}) $\Delta I/I_{CO}$ (%)
HbA	20	17	37
desHisβ146	21	17	39
desHisβ146−Tyrβ145	12	16	21
desArgα141	10	11	13
desArgα141−Tyrα140	2	1	2

[a] Intensity (I) was measured as the peak area, calculated by multiplying the fwhm by the peak height; the (ClO_4^-) peak height was used as reference. $\Delta I = I_{deoxy} - I_{CO}$, I_{deoxy}, and I_{CO} are the band intensities of deoxy and CO forms, respectively.

A similar pattern is seen for the Tyr difference bands, although the situation is complicated by the multiple contributions from the six Tyr residues per dimer. However, the T state upshift in the strong Y8a band, which gives rise to the sigmoidal difference band shape (Figure 4), is known to mainly arise from the α chain residues (*5*), and is attributed to the intersubunit H bond between Tyrα42 and Aspβ99 (Figure 1), which is lost in the R state (*1*, *39*−*40*). When

Table 4: Deconvolution of Tyr Y_i Bands in the 229-nm-Excited UVRR Spectra

	frequency (cm^{-1})								
	Y9a			Y7a			Y8a		
	deoxy	CO	Δ^a	deoxy	CO	Δ^a	deoxy	CO	Δ^a
HbA	1177.6	1176.4	1.2	1208.2	1206.8	1.4	1616.4	1614.9	1.5
desHisβ146	1177.3	1176.4	0.9	1207.5	1206.8	0.7	1615.9	1614.9	1.0
desHisβ146−Tyrβ145	1177.2	1176.5	0.7	1207.0	1205.9	1.1	1616.4	1615.2	1.2
desArgα141	1177.4	1176.2	1.2	1207.8	1207.4	0.4	1615.7	1614.8	0.9
desArgα141−Tyrα140	1177.5	1176.9	0.6	1207.3	1206.8	0.5	1615.6	1615.2	0.4

[a] Δ = deoxy-CO.

the parent Tyr bands are deconvoluted (Table 4), the Y8a upshift is seen to diminish from 1.5 cm^{-1} in Hb A, to about 1.0 cm^{-1} in desHisβ146, desHisβ146−Tyrβ145, and desArgα141, and to 0.4 cm^{-1} in desArgα141−Tyrα140. Thus, the response of Tyrα42 differs somewhat from that of Trpβ37. Removal of Hisβ146 affects the former but not the latter, whereas removal of Argα141 or of Hisβ146 plus Tyrβ145 affects Trpβ37 more than Tyrα42. Removal of both Argα141 and Tyrα140 nearly eliminate both the Trpβ37 and the Tyrα42 responses. However, some difference intensity is seen for this modification at both Y8a and Y9a, probably reflecting a contribution of the undeleted Tyrβ145 to the deoxy minus CO difference spectrum.

The assignment of the 1511 cm^{-1} difference band is currently uncertain. It had been assigned to the overtone of the very strong W18 band (755 cm^{-1}) (*1*), but isotope labeling of the Trp residues fails to shift this band, as would be required for the 2xW18 assignment (*5*). An alternative assignment to a protonated histidine residue was suggested, based on a 5 cm^{-1} shift in D_2O. A candidate residue was His β146, because its T state salt bridge raises its pK_a (*41*, *42*) and, therefore, the extent of protonation at pH 6.5. This possibility is now eliminated because the 1511 cm^{-1} difference intensity is unaltered by the removal of His β146 (Figure 4). Interestingly, the 1511 cm^{-1} difference intensity diminishes substantially in desArgα141, as well as in desArgα141−Tyrα140.

pH and IHP Effects on the UVRR Difference Spectra. Ligand binding to Hb is coupled to the binding of protons (Bohr effect) (*43*), and of anionic effectors such as 2,3-DPG (glycerol diphosphate) and IHP (inositol hexaphosphate) (*44*). The anions bind to the positively charged central cavity of the tetramer, particularly in the T state, for which the cavity size is optimal (*45*, *46*). The protons bind to residues whose pK_a is raised in the T state. Binding of anions, or of protons, therefore stabilizes the T state, relative to the R state. However, the T − R difference UVRR spectra of HbA have been shown not to depend on the pH or on the addition of IHP (*3*, *47*), indicating that the end-state structures themselves are unaltered by the binding event.

However, this is no longer the case when the C-terminal residues are deleted (Figures 5−8). Particularly striking is the appearance at high pH of negative difference signals, including a negative W3 band at the frequency (1558 cm^{-1}) of the interior Trp residues, α14 and β15 (*5*). These negative difference bands are recognizable as arising from R_{deoxy} molecules, Hb tetramers which are in the R quaternary state, but which have no ligand in one or more of the chains (*2*). The negative Trp bands are believed to reflect a collapse of the distal E helix toward the heme when ligand is absent,

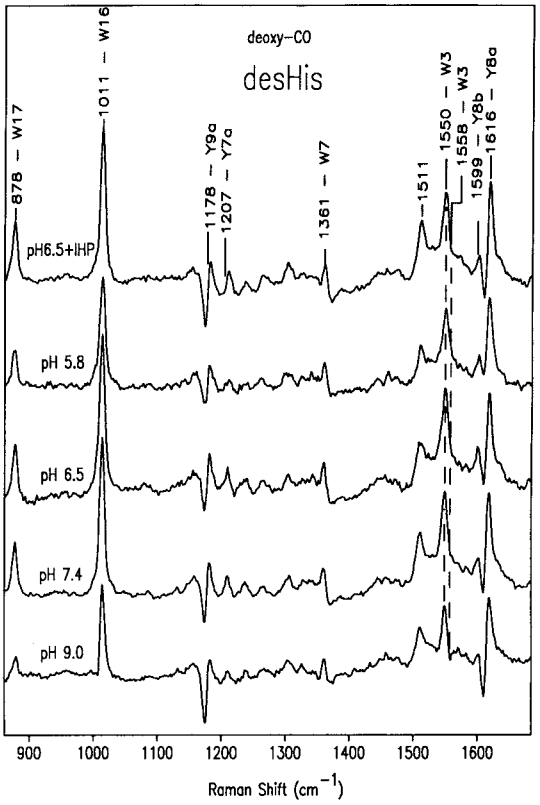

FIGURE 5: Deoxy minus CO difference spectra of desHisβ146 Hb at different pH values and with added IHP.

which weakens the H bonds between the Trpα14 and β15 residues on the A helices and the Thrα67 and Serβ72 residues on the E helices (Figures 2 and 13) (*2*). These H bonds are restored in the T state by a following motion of the A helices.

Thus, the appearance of R_{deoxy} difference spectra in the modified Hbs is direct evidence for conversion of deoxy tetramers to the R state at high pH. The R_{deoxy} difference bands are especially prominent for desArgα141 at pH 9 (Figure 7). At pH 7.4, the difference spectrum is a composite of the R_{deoxy} spectrum and the (partial) T − R difference spectrum seen at pH 6.5. Likewise, the desHisβ146−Tyrβ145 difference spectrum at pH 7.4 is a composite of the pH 6.5 T − R spectrum and an R_{deoxy} spectrum seen at pH 9.0, although the negative bands have lower amplitudes for this construct than for desArgα141. On the other hand, desHisβ146 shows a full T − R difference spectrum almost independent of pH. Only at pH 9.0 do the T − R signal intensities diminish somewhat, and a negative W3 band begins to appear at the interior Trp position, 1558 cm^{-1} (Figure 5), signaling the appearance of a small R_{deoxy}

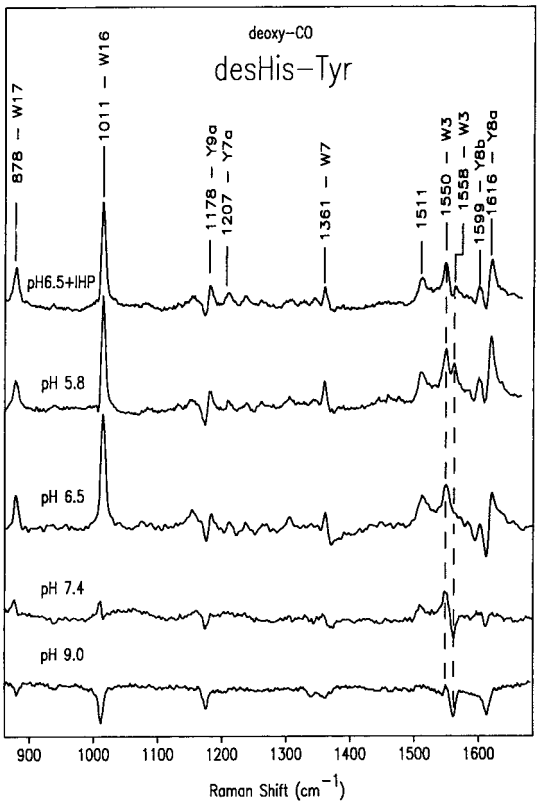

FIGURE 6: As Figure 6, but for desHisβ146−Tyrβ145 Hb.

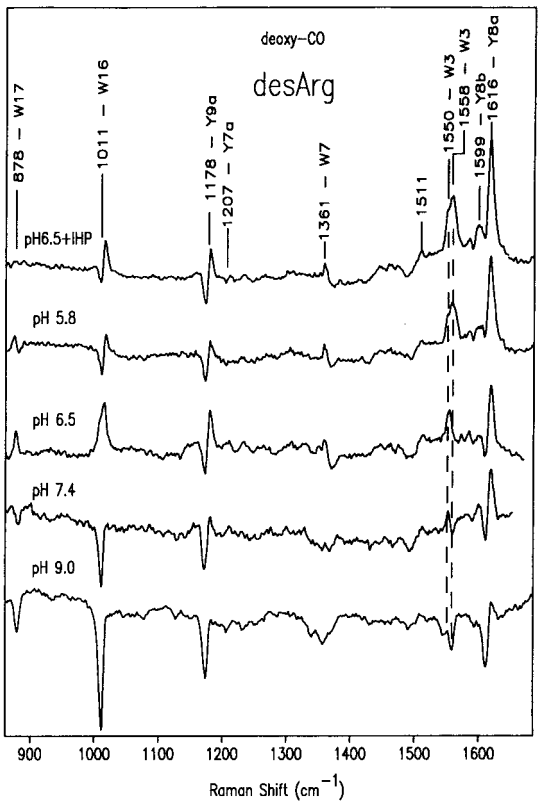

FIGURE 7: As Figure 6, but for desArgα141 Hb.

population. However, desArgα141−Tyrα140 does *not* give a R_{deoxy} spectrum, even at pH 9.0. Its difference spectrum is close to baseline and is essentially independent of pH. We infer that this modification is severe enough to eliminate the quaternary constraints on the R as well as the T state.

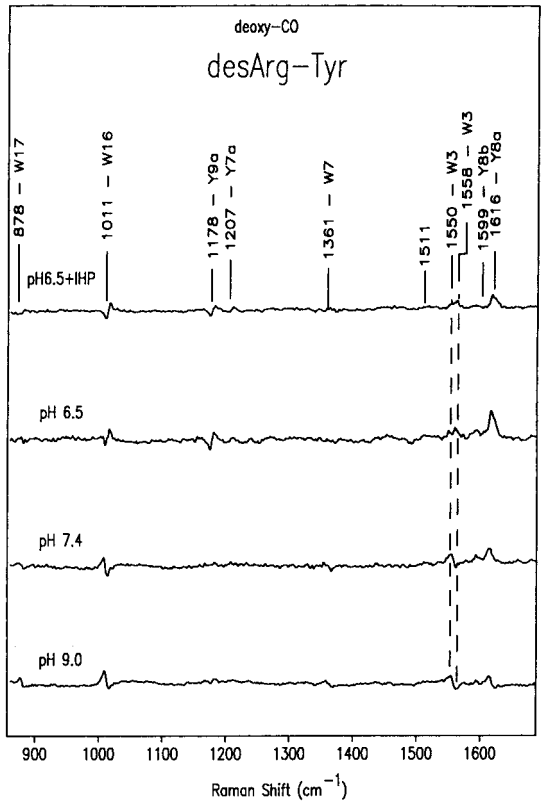

FIGURE 8: As Figure 6, but for desArgα141−Tyrα140 Hb.

When the pH is lowered to 5.8, or when IHP is added to the pH 6.5 solution, the T − R difference signals are not significantly augmented, contrary to expectation. However, a new signal is superimposed on the T − R difference spectrum for the intermediate pair of modifications, desHisβ146−Tyrβ145 and desArgα141 (Figures 6 and 7), namely a *positive* W3 difference band at the interior Trp position, 1558 cm^{-1}. This positive signal implies *strengthened* H bonds for Trpα14 and/or β15 in the T state, in contrast to the weakened H bonds in the R_{deoxy} forms. This new signal is not seen, however, for the minimally perturbed desHisβ146 (Figure 5), nor for the maximally perturbed desArgα141−Tyrα140 (Figure 8). Thus, the strengthened interior Trp H bonds seem to arise when a moderately perturbed T state is subject to extra T stabilization (IHP or lowered pH). Instead of restoring the $\alpha_1\beta_2$ contacts, the effector binding appears to compress the A helix against the E helix, strengthening the interhelix H bonds.

Structural Perturbations. Further insight into the molecular interactions which are perturbed by the C-terminal deletions can be gained by subtracting the spectra of the modified Hbs from that of Hb A (Figure 9). As expected, deletion of Hisβ146 is the least perturbing modification. A slight intensity loss is seen for Y8a, in both deoxy and CO forms, probably signaling some weakening of the H bond formed by the penultimate Tyrβ145 residue when the buttressing effect of Hisβ146 is lost.

In desHisβ146−Tyrβ145, substantial intensity is lost for all of the Y bands, because of the deletion of one out of the six Tyr residues per dimer. But, in addition, significant Trp difference signals appear, and a negative W3 difference band is seen at the *interior* Trp position, 1558 cm^{-1}, signaling a weakening of the A−E helix contacts in Hb A, relative to

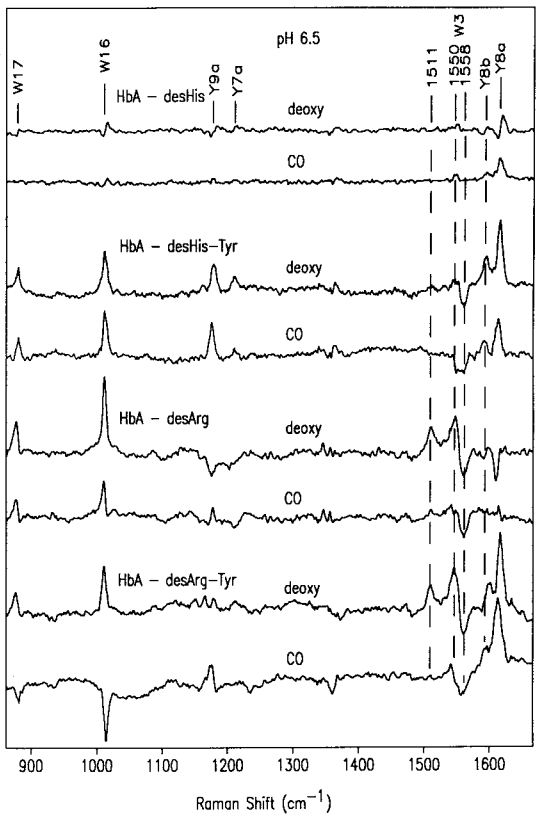

FIGURE 9: Difference spectra between native and modified Hbs, in deoxy and CO forms, at pH 6.5.

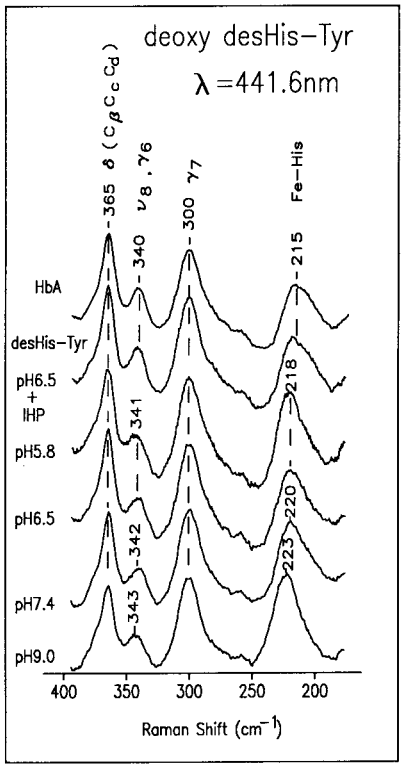

FIGURE 10: RR spectra excited at 441.6 nm of deoxyHb (1 mM in heme) in the low-frequency region, showing the Fe−His stretching band, and nearby porphyrin bands (see ref *50* for assignments). Hb A is compared with desHisβ146−Tyrβ145 Hb at different pH values, and with added IHP.

desHisβ146−Tyrβ145. Because the same negative band occurs for both deoxy and CO forms, there is no difference signal of the interior Trp residues in the deoxy minus CO spectra, at pH 6.5 (Figure 6), although a positive deoxy minus CO W3 band at 1558 cm^{-1} does appear upon lowering the pH to 5.8 or adding IHP, as discussed above. We infer that the A−E helix contacts are strengthened in *both* the R and the T state by the deletion of Hisβ146 and Tyrβ145 and that these contacts are further strengthened in the T state by protonation or IHP addition. Exactly the same effect is seen for desArgα141, which shows negative 1558 cm^{-1} bands in the difference spectra relative to Hb A (Figure 9), and positive bands in the deoxy minus CO difference spectra at pH 5.8 or in the presence of IHP (Figure 6). Likewise, desArgα141−Tyrα140 produces a negative 1558 cm^{-1} band, relative to Hb A (Figure 9), but in this case, no positive deoxy minus CO difference band is detected (Figure 8). Thus, all three of the more perturbing modifications appear to have stronger A−E contacts than Hb A, but the T state augumentation seen at low pH or with IHP addition for desHisβ146−Tyrβ145 and desArgα141 does not occur for desArgα141−Tyrα140.

Deletion of Argα141 or of Argα141 and Tyrα140 produces significant intensity loss at the Trpβ37 W3 position (1550 cm^{-1}) in the deoxy form (Figure 9), reflecting the marked weakening of the $\alpha_1\beta_2$ contacts in the T state (Figure 4).

Visible RR Spectra and the Fe−His Bond. The effect of the C-terminal deletions on the strength of the Fe−His bond was monitored via RR spectra obtained in resonance with the heme Soret band, which enhances the Fe−His stretching vibration at ~220 cm^{-1} in deoxy-heme proteins (*26*). In Hb A, this vibration gives rise to a broad band at 215 cm^{-1}, which is a composite of α and β chain contributions (*26*, *27*). It is well-known that weakening of the T state constraints raises this frequency toward the relaxed value, 223 cm^{-1}, observed in deoxy-myoglobin or in isolated Hb chains (*48*, *49*). All of the C-terminal deletions produce upshifts in the 215 cm^{-1} band, the extent of the shift increasing with pH; the spectra are illustrated in Figure 10 for desHisβ146−Tyrβ145. In addition, one can observe a smaller upshift and broadening of the 340 cm^{-1} band, which is a composite of the ν_8 porphyrin skeletal mode and the γ_6 out-of-plane mode (*50*).

To quantify the pH effect on the Fe−His band, we subtracted the most relaxed spectrum, that of desArgα141−Tyrα140 or desHisβ146−Tyrβ145 at pH 9.0, from each of the other spectra (Figure 11). This is a more discriminating procedure than locating the band maximum, because the shape of the band changes along with the position. The shape change reflects the greater Fe−His sensitivity in the α than the β chains to protein alterations (*26*, *49*). Both subunits have essentially the same relaxed frequencies, ~223 cm^{-1}, but the α chains show larger downshifts than the β chains under T-stabilizing conditions, and they show greater variability within the T state (*49*, *51*, *52*). Our difference spectra all show peaks at 203 cm^{-1} and troughs at 230 cm^{-1}, with well-behaved isosbetic points for different pH values, suggestive of a two component system. The two components can be modeled with positive and negative Gaussian bands (15 cm^{-1} half-width) at 205 and 230 cm^{-1}, respectively. We interpret the two components as being associated with α chains having the most and least strain on the Fe−His bond.

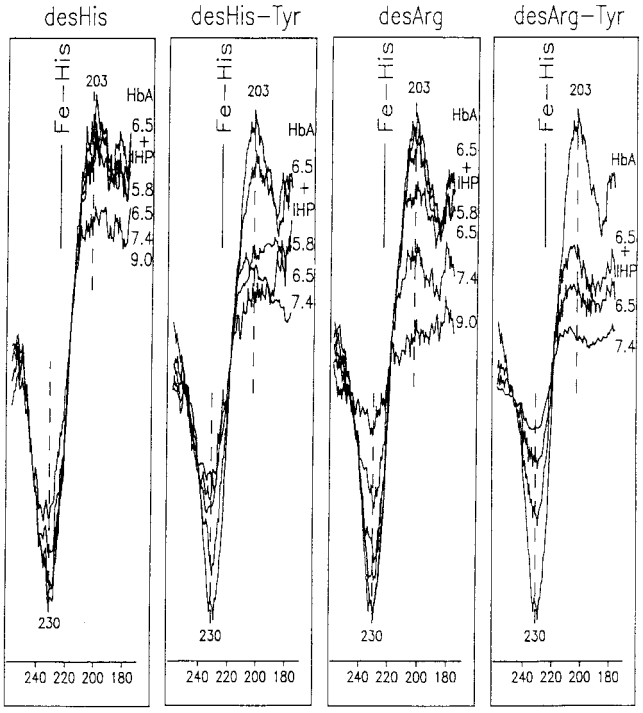

FIGURE 11: Difference spectra in the region of the Fe−His band between modified Hbs under the indicated conditions and fully relaxed spectra of desHisβ146−Tyrβ145 or desArgα141−Tyrα140 at pH 9.0.

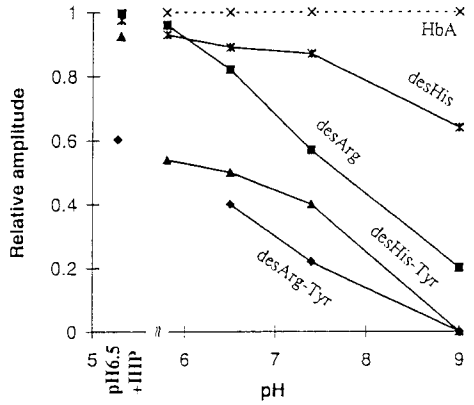

FIGURE 12: The pH dependence of peak-trough difference amplitudes from Figure 11, normalized to the amplitude of deoxy HbA. The larger the amplitude, the lower the Fe−His frequency.

However, the pH titration curves are far from being sigmoidal (Figure 12). The peak-to-trough amplitude approaches that of Hb A as the pH is lowered, and IHP is added, and trends gradually downward at high pH. The near-linearity of the titration curves implies multiple contributions from groups with variable pK_as. The relaxation from Hb A behavior increases in the order desHisβ146 < desArgα141 < desHisβ146−Tyrβ145 < desArgα141−Tyrα140. This is the same order as observed for functional perturbations (Table 1).

It is important to note that the Fe−His shift is not coextensive with quaternary structure changes. Thus, desHisβ146 shows significant Fe−His relaxation at pH 9 but very little R_{deoxy} population (Figure 4), while in desArgα141 and, especially, desHisβ146−Tyrβ145, substantial Fe−His relaxation is evident even at pH 6.5, whereas R_{deoxy} molecules only appear at higher pH (Figures 6 and 7). We infer that Fe−His relaxation results from the weakening of T state contacts, as well as from a switch to the R state, which only begins at higher pH. As expected, the Fe−His bond is most relaxed in desArgα141−Tyrα140, where no significant quaternary constraints are detectable in the UVRR spectra (Figure 9). Nevertheless, the Fe−His relaxation is partially reversed at low pH and in the presence of IHP, suggesting partial conversion to a strained structure, even in this severely perturbed Hb.

DISCUSSION

The results of chemical modification reveal a multiplicity of linkages between structure and function that are hidden in native Hb by the concertedness of the allosteric transition. The UVRR spectra of Hb A do not depend on the concentration of protons or IHP, in either the deoxy or fully ligated states (*3*, *47*), even though these effectors strongly influence both the kinetics and thermodynamics of ligand binding (*44*, *53*). This observation is consistent with the two end-state structures being unaltered by effector binding, although their relative stabilities are strongly affected. The C-terminal deletions confirm that the T quaternary structure is destabilized at high pH and demonstrate that the R structure can become the lower energy one, even in the absence of ligand binding. However, they also reveal considerable plasticity within these structures, once the C-terminal constraints are removed.

Figure 13 gives a schematic view of the critical interactions that are affected by the chemical modifications, as discussed in the following sections.

R State. UVRR spectroscopy has revealed an important conformational change within the R quaternary structure, which depends on the occupancy of the ligand-binding site (*2*). Whenever one or more of these sites is unoccupied, but the tetramer remains in the R state, then the difference spectrum, relative to the fully ligated species, contains a characteristic set of negative Trp and Tyr bands. This spectrum has been seen for tri-ligated cyanomet valency hybrid Hbs (*54*) and for diligated Co, Fe hybrid Hbs (*2*), as well as for the 50 ns intermediate of HbCO photodissociation, in which CO molecules have been expelled from the heme pockets but the tetramer remains in the R structure (*2*, *3*). The structural interpretation of this spectrum rests on the fact that the negative W3 band is at the frequency (1558 cm^{-1}) of the interior Trp residues, α14 and β15, rather than at the frequency (1548 cm^{-1}) of the interfacial Trp residue, β37. These interior residues are on the A helices, but are H bonded to acceptor side chains of residues (Thrα67, Serβ72) on the adjacent E helices (Figures 2 and 13). The loss of intensity upon deligation is consistent with weakening of these H bonds (which shifts the excitation profiles to higher energy), as a consequence of E helix displacement toward the heme, when the distal pocket no longer contains ligand.

The appearance of the R_{deoxy} spectrum at pH 9 upon C-terminal deletion is direct evidence for conversion to the R state in the absence of ligand. But, in addition, we observe a negative 1558 cm^{-1} band when the spectra of the modified Hbs are subtracted from the spectra of unmodified Hb A, in the presence or absence of ligand (Figure 9). Thus, the H bonds of the interior Trp residues are strengthened by the modifications, implying that the A−E helix separation is diminished, regardless of the occupancy of the heme pockets.

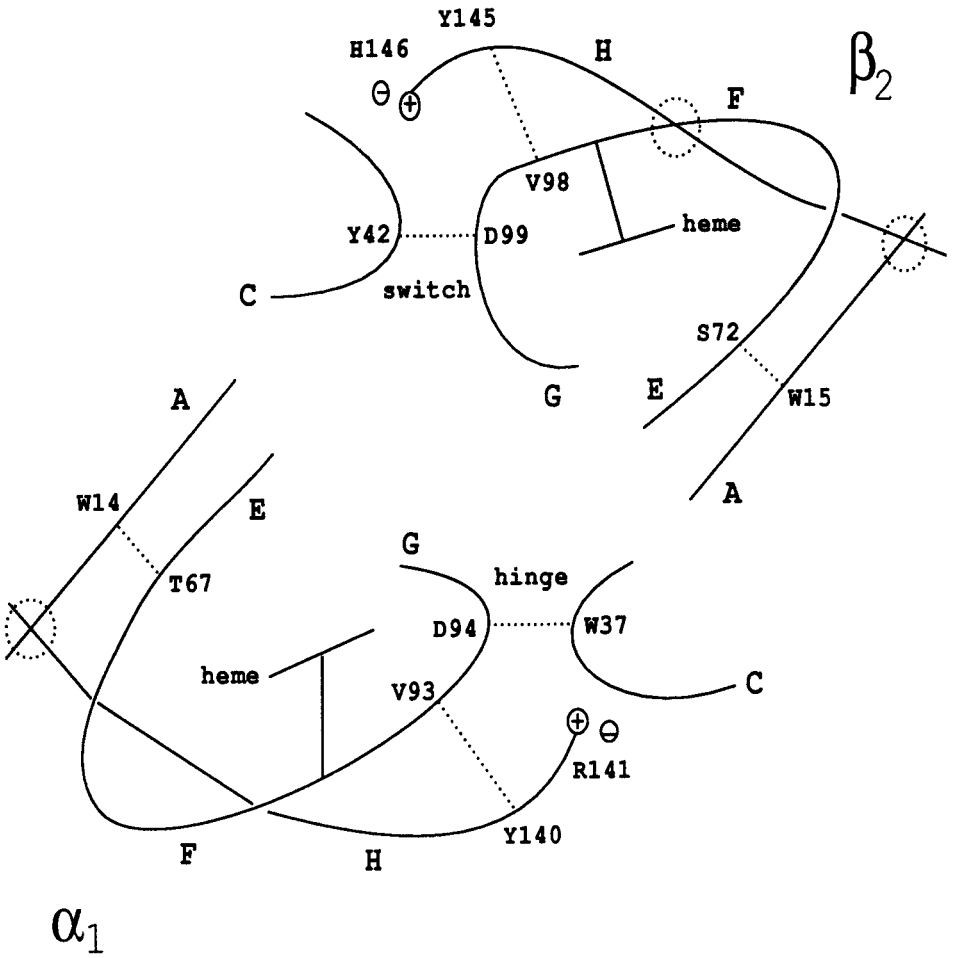

FIGURE 13: Schematic view of tertiary and quaternary contacts in deoxy Hb, showing helices, H bonds (···), salt-bridges (+, −), and contacting residues. Removal of the Argα141 salt-bridge loosens the α chain H-helix, allowing the A-helix to approach the E-helix; effector binding strengthens this contact further leaving the $\alpha_1\beta_2$ contacts weakened but nevertheless restoring tension to the Fe−His linkage. The additional removal of Tyrα140 unmoors the H-helix and loosens all quaternary contacts, but still permits partial restoration of the Fe−His tension by effectors. Loss of Hisβ146 has a smaller effect because of additional H−F interhelix H bonds in the β chain (circle). Only at pH 9.0 is there evidence of a small R-deoxy population, although the Fe−His tension is somewhat relaxed. Additional removal of Tyrβ145 weakens, but does not destroy the T-contacts. The Fe−His tension is relaxed more than by Argα141 removal but less than Argα141 and Tyrα140 removal.

What is the molecular origin of this effect? The C-terminal residues are far in sequence space from either the A or E helices, but they anchor the H helix, which is in contact with both the F and A helices (Figures 2 and 13). In both chains, there are significant H−A interhelix salt bridges or H bonds: Lysα127...Aspα6, Aspα6...Serα124...Asnα9, and Tyrβ130...Valβ11 (C═O). Thus, the H helix serves as a scaffold for the A helix. Loss of the H helix anchors loosens the scaffold, and permits collapse of the A helix toward the E helix, thus, strengthening the interior Trp H bonds. We can also explain why this effect is pronounced for desArgα141, but barely detectable for desHisβ146. In the β chains, there also exist a H−F interhelix salt bridge, Lysβ144−Gluβ90, and a H-bond network, Lysβ144−Serβ89−Leuβ141, which can preserve the scaffold even when the Hisβ146 anchor is missing; the α chains do not have this secondary anchor (Figures 2 and 13). However, removal of Tyrβ145 as well as Hisβ146, overwhelms the secondary anchor and allows the A helix to collapse even in the β chains; Tyrβ145 also buttresses the scaffold by H bonding to a F-helix residue Valβ98. Similarly, Tyrα140 buttresses the α-chain scaffold by H bonding to the F-helix residue Valα93. When Tyrα140 is removed along with Argα141, the constraints are so loosened that the A−E helix separation no longer increases when ligands are removed in the R state (no R_{deoxy} signal at pH 9) (Figure 8).

T State. When the pH is lowered from 9, the R_{deoxy} signals for the modified Hbs are replaced by the classical T − R difference signals (Figure 4), which reflect the formation of the Trpβ37...Aspα94 and Tyrα42...Aspβ99 H bonds across the $\alpha_1\beta_2$ interface (Figures 1 and 13). The former H bond is affected greatly by removal of Argα141, but not by removal of Hisβ146 (Table 3), while the strength of the perturbation is reversed for the latter H bond (Table 4). This reversal can be explained by the spatial arrangement of the $\alpha_1\beta_2$ interface (Figures 1 and 13); the Tyrα42...Aspβ99 H bond is near Hisβ146, while the Trpβ37...Aspα94 H bond is near Argα141. Removal of one or the other anchoring salt bridge allows the nearby interfacial contact to weaken. We note that Englander and co-workers also found localization of interfacial contacts, since removal of Argα141 had no significant effect on H/D exchange rates at the β C-terminus (*55*). When Tyrβ145 is removed along with Hisβ146, the more distant Trpβ37...Aspα94 H bond is also attenuated, but not by as much as when only Argα141 is removed. Both interfacial contacts are lost when Tyrα140

as well as Argα141 is removed, probably because of the complete unmooring of the α-chain H helix, as discussed in the preceding section.

Surprisingly, the interfacial contacts are not restored by adding IHP or lowering the pH to 5.8, even though these conditions do increase the tension on the Fe−His bond (see next section). Instead, the interior Trp H bonds are strengthened (positive 1558 cm^{-1} bands in the deoxy-CO difference spectra) (Figures 6 and 7), signaling a further reduction in the A−E helix separation. Thus, the T state effectors do not fully recover the T quaternary structure, but they compensate by drawing the A toward the E helix, presumably via the loosened H helices. This effect is seen for the moderate perturbations, desHisβ146−Tyrβ145 and desArgα141, but not for the severe perturbation, des Argα141−Tyrα140, whose UVRR spectrum shows no effect of IHP addition (Figure 8).

Fe−His Strain Gauge. Despite all these complexities, the Fe−His stretching frequency faithfully follows the functional perturbations (Figure 12 and Table 1). The increase in ligand affinity and the loss of both cooperativity and the Bohr effect are greatest for desArgα141−Tyrα140 and least for desHisβ146, while they are greater for desHisβ146−Tyrβ145 than for desArgα141. The Fe−His frequency increases in the same order. This behavior is consistent with previous studies showing a positive correlation between ligand affinity and the Fe−His frequency in myoglobins and hemoglobins (*26*). The frequency decreases when Fe−His bond is stretched (lower force constant) and the propensity for ligation is diminished. The molecular basis for this tension is still a matter of speculation; tilting (*27*, *56*) and/or reorientation (*57*) of the proximal imidazole, as well as H bonding to a backbone carbonyl (*58*), have all been suggested as possible elements in the mechanism. Any or all of these mechanisms are consistent with our results. Loss of the H helix anchors at the C-termini, and especially loss of the F−H interhelix H bonds provided by the penultimate tyrosines (*40*), will allow relaxation of the F helix, and of the proximal imidazole orientation, as well as its H bond with the nearby leucine carbonyls (Figure 2). The effects are bigger for the α chain, as is also the case for A−E helix collapse, because of the absence of additional H−F interhelix H bonds.

However, the present results show that quaternary structure is not the only correlate of the Fe−His bond strength. For all the modified Hbs, the Fe−His frequency decreases smoothly as the pH is lowered from 9, although R_{deoxy} molecules are not detected below pH 7.4. The Fe−His frequency is lowered further upon IHP addition, even though the effect of IHP is not to restore the $\alpha_1\beta_2$ interface, but rather to compress the A and E helices. Particularly striking is the behavior of desArgα141, whose Fe−His tension is equivalent to that of Hb A when IHP is added or the pH is lowered to 5.8, even though the deoxy minus CO UVRR difference spectra differ markedly. Thus, tension can be exerted by different conformations within the T quaternary structure. Likewise, there is variation in the R quaternary structure, since the desArgα141 Fe−His frequency is lower than that of desHisβ146−Tyrβ145, even at pH 9, where no significant T population remains. Even for desArgα141−Tyrα140, the Fe−His frequency diminishes as the pH is lowered from 9 and IHP is added, although there is no evidence of T formation under any conditions. We conclude that the Fe−His bond is a general purpose strain gauge, which can respond to many structural alterations, and not just the quaternary arrangement of the subunits.

It is also notable that the titration curves for the Fe−His band are almost linear over a range of three pH units (Figure 12). They cannot be described by one or two pK_a values. These shapes are consistent with a multiplicity of contributors to the Bohr effect, involving groups with a range of pK_a values (*59*, *60*). Moreover, deletion of Hisβ146, which is known to be an important Bohr contributor (*41*, *42*), does not produce behavior that is qualitatively different from the other deletions.

CONCLUSIONS

What implications do the chemically modified Hbs have with respect to structure and function in native Hb? They clearly demonstrate that the protein structure is somewhat plastic in both quaternary structures when the C-terminal anchors are removed. But is the native protein plastic? The spectra give no indication of structure change with solution conditions (pH, IHP), when Hb A is fully ligated or fully deligated. Yet, there must be plasticity in the intermediately ligated forms, contrary to the classical two-state model. The clearest evidence for this comes from Mozzarelli et al.'s elegant measurements of oxygen affinity in single crystals of Hb (*61*, *62*). Soaking the crystals in IHP, or in another effector molecule, bezafibrate, did not alter the affinity, although these effectors are known to lower the T state affinity 10−30-fold in solution. Thus, the crystal contacts inhibit a T state relaxation upon binding of the first ligand, which is permitted in solution, but is counteracted by T state effectors. This relaxation must alter the structure to some extent. We also note the recent report of Bonaventura et al. (*63*) that sulfhydryl reactivity is diminished by anion binding to deoxy HbA, implying a loss of conformational flexibility within the T state. In addition, Ackers and co-workers have reported thermodynamic measurements of tetramer dissociation, which point toward alternative structures depending on the arrangement of ligands within the tetramer (*64*). In particular, they find that two ligands are more strongly bound when they occupy sites within the same $\alpha\beta$ dimer, than when the sites lie across the dimer interface. Consistent with this finding, the UVRR difference spectra are different in character when two cyanomet hemes occupy sites within a dimer (asymmetric diligated hybrid) than when they occupy two α or two β chains (symmetric diligated hybrids) (*52*, *54*). The latter give mixtures of T and R_{deoxy} contributions, while the former show attenuated T signals but no R_{deoxy} signals. Again, this is evidence for plasticity within the T quaternary structure, this time depending on the arrangement of two ligands.

Of course the degree of structural plasticity need not be the same for chemical modification as it is for partial ligation of the native structure. Nevertheless, it seems likely that the nature of the conformation changes induced by the C-terminal deletions will lend insight into the structural transformations of the native protein.

ACKNOWLEDGMENT

We thank Mr. Xuehua Hu and Dr. Xiaojie Zhao for helpful discussions. We also thank electrospray mass spectrometry

facilities at U.C. San Francisco (NIH NCRR BRTP RR01614), the University of Washington (NIH P41RR0954), and Princeton University (NIH 1S10RRO) for the ESMS measurements of the modified hemoglobins.

REFERENCES

1. Rodgers, K. R., Su, C., Subramaniam, S., and Spiro, T. G. (1992) *J. Am. Chem. Soc. 114*, 3697.
2. Rodgers, K. R., and Spiro, T. G. (1994) *Science 265*, 1697.
3. Jayaraman, V., Rodgers, K. R., Mukerji, I., and Spiro, T. G. (1995) *Science 269*, 1843.
4. Hu, X., Frei, H., and Spiro, T. G. (1996) *Biochemistry 35*, 13001.
5. Hu, X., and Spiro, T. G. (1997) *Biochemistry 36*, 15701.
6. Perutz, M. F. (1970) *Nature 228*, 726.
7. Baldwin, J. M., and Chothia, C. (1979) *J. Mol. Biol. 129*, 175.
8. Baldwin, J. M. (1980) *J. Mol. Biol. 136*, 103.
9. Shaanan, B. (1983) *J. Mol. Biol. 171*, 31.
10. Fermi, G., Perutz, M. F., Shaanan, B., and Fourme, R. (1984) *J. Mol. Biol. 175*, 159.
11. Kilmartin, J. V., and Wootton, J. F. (1970) *Nature 228*, 766.
12. Kilmartin, J. V., and Hewitt, J. A. (1971) *Cold Spring Harbor Symp. Quantum Biol. 36*, 311.
13. Kilmartin, J. V., Hewitt, J. A., and Wootton, J. F. (1975) *J. Mol. Biol. 93*, 203.
14. Hewitt, J. A., and Gibson, Q. H. (1973) *J. Mol. Biol. 74*, 489.
15. Moffat, K., Olson, J. S., and Gibson, Q. H. (1973) *J. Biol. Chem. 248*, 6387.
16. Bonaventura, J., Bonaventura, C., Brunori, M., Giardina, B., Antonini, E., Bossa, F., and Wyman, J. (1974) *J. Mol. Biol. 82*, 499.
17. Imai, K. (1973) *Biochemistry 5*, 788.
18. Bonaventura, J., Bonaventura, C., Giardina, B., Antonini, E., Brunori, M., and Wyman, J. (1972) *Proc. Nat. Acad. Sci. U.S.A. 8*, 2174.
19. Perutz, M. F., and TenEyck, L. F. (1971) *Cold Spring Harbor Symp. Quantum Biol. 36*, 295.
20. Brunori, M., Noble, R. W., Antonini, E., and Wyman, J. (1966) *J. Biol. Chem. 241*, 5338.
21. Tyuma, I., Benesch, R. E., and Benesch, R. (1966) *Biochemistry 5*, 2957.
22. Mills, F. C., Johnson, M. L., and Ackers, G. K. (1976) *Biochemistry 15*, 5350.
23. Atha, D. H., and Riggs, A. (1976) *J. Biol. Chem 251*, 5537.
24. Moffat, K., Olson, J. S., and Gibson, Q. H. (1973) *J. Biol. Chem. 18*, 6387.
25. Van Beek, G. G. M., Zuiderweg, E. R. P., and De Bruin, S. H. (1978) *Eur. J. Biochem. 92*, 309.
26. Kitagawa, T. (1987) in *Biological Applications of Raman Spectroscopy* (Spiro, T. G. Ed.) Vol. 3, pp 97, John Wiley & Sons, New York.
27. Friedman, J. M., Rousseau, D. L., Ondrias, M. R., and Stepnoski, R. A. (1982) *Science 218*, 1244.
28. Spiro, T. G. (1985) *Adv. Protein Chem. 37*, 111.
29. Harada, I. and Takeuchi, I. (1986) in *Spectroscopy of Biological Systems* (Clark, R. J., and Hester, R. E., Eds.) pp 113, John Wiley & Sons, New York.
30. Austin, J., Jordan, T., and Spiro, T. G. (1993) *Biomolecular Spectroscopy, Part A* (Clark, R. J. H., & Hester, R. E., Eds.) pp 55, John Wiley & Sons, New York.
31. Antonini, E., and Brunori, M. (1971) *Hemoglobin and Myoglobin in Their Reactions with Ligands*, pp 2−4, North-Holland Publishing Co., Amsterdam.
32. Riggs, A. (1981) *Methods Enzymol. 76*, 5.
33. Kilmartin, J. V. (1981) *Methods Enzymol. 76*, 167.
34. Bucci, E., and Fronticellic, C. (1965) *J. Biol. Chem. 240*, 551.
35. Bucci, E. (1981) *Methods Enzymol. 76*, 97.
36. Yip, Y. K., Waks, M., and Beychok, S. (1977) *Proc. Natl. Acad. Sci. U.S.A. 74*, 64.
37. Ikeda-Saito, M., Inubushi, T., and Yonetani, T. (1981) *Methods Enzymol. 76*, 113.
38. Miura, T., Takeuchi, H., and Harada, I. (1989) *J. Raman Spectrosc. 20*, 667.
39. Nagai, M., Imai, K., Kaminaka, S., Mizutani, Y., and Kitagawa, T. (1996) *J. Mol. Struct. 379*, 65.
40. Huang, S., Peterson, E. S., Ho, C., and Friedman J. M. (1997) *Biochemistry 36*, 6197.
41. Kilmartin, J. V., Breen, J. J., Roberts, G. C. K., and Ho, C. (1973) *Proc. Natl. Acad. Sci. U.S.A. 70*, 1246.
42. Matsukawa, S., Itatani, Y., Mawatari, K., Shimokawa, Y., and Yoneyama, Y. (1978) *J. Biol. Chem. 259*, 11479.
43. Bohr, C., Hasselbalch, K., and Krogh, A. (1904) *Skand. Arch. Physiol. 16*, 402.
44. Marden, M. C., Bohn, B., Kister, J., and Poyart, C. (1990) *Biophys. J. 57*, 397.
45. Arnone, A. (1972) *Nature 237*, 146.
46. Arnone, A., and Perutz, M. F. (1974) *Nature 249*, 34.
47. Jayaraman, V., Rodgers, K. R., Mukerji, I., and Spiro, T. G. (1993) *Biochemistry 32*, 4547.
48. Hu, S., Smith, K. M., and Spiro, T. G. (1996) *J. Am. Chem. Soc. 118*, 12638.
49. Nagai, K., and Kitagawa T. (1980) *Proc. Natl. Acad. Sci. U.S.A. 77*, 203.
50. Jayaraman, V., and Spiro. T. G. (1996) *Biospectroscopy 2*, 311.
51. Ondrias, M. R., Roussesu, D. L., Kitagawa, T., Ikeda-Saito, M., Inubushi, T., and Yonetani, T. (1982) *J. Biol. Chem. 257*, 8766.
52. Mukerji, I., and Spiro, T. G. (1994) *Biochemistry 33*, 13132.
53. Perutz, M. F. (1990) *Annu. Rev. Physiol. 52*, 1.
54. Jayaraman, V., and Spiro, T. G. (1995) *Biochemistry 34*, 4511.
55. Louie, G., Tran, T., Englander, J. J., and Englander S. W. (1988) *J. Mol. Biol. 201*, 755.
56. Friedman, J. M., Scott, T. M., Stepnoski, R. A., Ikeda-Saito, M., and Yonetani, T. (1983) *J. Biol. Chem. 258*, 10564.
57. Bangharoenpaurpong, O., Schomacker, K. T., and Champion, P. M. (1984) *J. Am. Chem. Soc. 106*, 5688.
58. Stein P., Mitchell, M., and Spiro, T. G. (1980) *J. Am. Chem. Soc. 102*, 7797.
59. Perutz, M. F., Kilmartin, J. V., Nishikura, K., Fogg, J. H., Butler, P. J. G., et al. (1980) *J. Mol. Biol. 138*, 649.
60. Ho, C., and Peruss, J. R. (1994) *Methods Enzymol. 232*, 97.
61. Mozzarelli, A., Rivetti, C., Rossi, G. L., Henry, E. R., and Eaton, W. A. (1991) *Nature 351*, 416.
62. Mozzarelli, A., Rivetti, C., Rossi, Eaton, W. A.; G. L., Henry, E. R. (1997) *Protein Sci. 6*, 484.
63. Bonaventura, C., Tesh, S., Faulkner K. M., Kraiter, D., and Crumbliss, A. L. (1998) *Biochemistry 37*, 496.
64. Ackers, G. K., Doyle, M. L., Myers, D., and Daugherty, M. A. (1992) *Science 255*, 54.

BI980295H